Chirp and error rate analyses of an optical-injection gain-switching VCSEL based all-optical NRZ-to-PRZ converter

Chia-Chi Lin[1], Hao-Chung Kuo[2], Peng-Chun Peng[3], and Gong-Ru Lin[1*]

[1]*Institute of Photonics and Optoelectronics, Department of Electrical Engineering, National Taiwan University No.1 Roosevelt Rd. Sec. 4, Taipei 106, Taiwan R.O.C.*
[2]*Department of Photonics, National Chiao Tung University*
[3]*Department of Applied Materials and Electro-Optical Engineering, National Chi Nan University*
**Corresponding and Reprint E-mail: grlin@ntu.edu.tw*

Abstract: Optically injection-locked single-wavelength gain-switching VCSEL based all-optical converter is demonstrated to generate RZ data at 2.5 Gbit/s with bit-error-rate of 10^{-9} under receiving power of -29.3 dBm. A modified rate equation model is established to elucidate the optical injection induced gain-switching and NRZ-to-RZ data conversion in the VCSEL. The peak-to-peak frequency chirp of the VCSEL based NRZ-to-RZ is 4.5 GHz associated with a reduced frequency chirp rate of 178 MHz/ps at input optical NRZ power of -21 dBm, which is almost decreasing by a factor of 1/3 comparing with chirp on the SOA based NRZ-to-RZ converter reported previously. The power penalty of the BER measured back-to-back is about 2 dB from 1 Gbit/s to 2.5 Gbit/s.

OCIS codes: (060.2330) Fiber optics communications; (250.5980) Semiconductor optical amplifiers; (200.4560) Optical data processing; (320.5540) Pulse shaping

References and links

1. H. Li and K. Iga, "*Vertical-Cavity Surface-Emitting Laser Devices*," (Berlin, New York, Springer, 2003), Chaps. 2, 3.
2. T. Fishman and A. Hardy, "Injection- locking analysis of vertical-cavity laser arrays," J. Opt. Soc. Am. B **16**, 38-45 (1999).
3. T. Fishman and A. Hardy, "Effect of spatial hole burning on injection-locked vertical-cavity surface-emitting laser arrays," Appl. Opt. **39**, 3108-3114 (2000).
4. J. Y. Law, G. H. M. van Tartwijk, and G. P. Agrawal, "Effects of transverse-mode competition on the injection dynamics of vertical-cavity surface-emitting lasers," Quantum Semiclasic. Opt. **9**, 737-47 (1997).
5. H. Li, T. L. Lucas, J. G. McInerney, M. W. Wright, and R. A. Morgan, "Injection locking dynamics of vertical cavity semiconductor lasers under conventional and phase conjugate injection," IEEE J. Quantum Electron. **32**, 227-235 (1996).
6. D. L. Boiko, G. M. Stephan, and P. Besnard, "Fast polarization switching with memory effect in a vertical cavity surface emitting laser subject to modulated optical injection," J. of Appl. Phys. **86**, 4096-4099 (1999).
7. Y. Onishi, N. Nishiyama, C. Caneau, F. Koyama, and C. E. Zah, "Optical Inverter using a Vertical-Cavity Surface-Emitting Laser with External Light Injection," Proc. IEEE LEOS Annual Meeting, (2003).
8. L. Li, "A unified description of semiconductor lasers with external light injection and its application to optical bistability," IEEE J. Quantum Electron. **30**, 1723-1726 (1994).
9. K. Hasebe and F. Koyama, "Modeling of all-optical-signal processing devices based on two-mode injection-locked vertical-cavity surface-emitting laser," Jpn. J. Appl. Phys. **45**, 6697-6703 (2006).
10. Y. C. Chang, Y. H. Lin, J. H. Chen, and G.-R. Lin, "All-optical NRZ-to-PRZ format transformer with an injection-locked Fabry-Perot laser diode at unlasing condition," Opt. Express **12**, 4449-4456 (2004).
11. D. Norte and A. E. Willner, "Demonstration of an all-optical data format transparent WDM-to-TDM network node with extinction ratio enhancement for reconfigurable WDM networks," IEEE Photon. Technol. Lett. **8**, 715-717 (1996).
12. C. G. Lee, Y. J. Kim, C. S. Park, H. J. Lee, and C.-S. Park, "Experimental demonstration of 10-Gb/s data format conversions between NRZ and RZ using SOA-loop-mirror," J. Lightwave Technol. **23**, 834-841 (2005).

#89943 - $15.00 USD Received 20 Nov 2007; revised 24 Jan 2008; accepted 2 Feb 2008; published 25 Mar 2008

13. L. X. Wang, B.C. Baby, V. Glesk, and I. Prucnal, "All-optical data format conversion between RZ and NRZ based on a Mach-Zehnder interferometric wavelength converter," IEEE Photon. Technol. Lett. **15**, 308-310 (2003).
14. A. Reale, P. Lugli, and S. Betti, "Format conversion of optical data using four-wave mixing in semiconductor optical amplifiers," IEEE J. Sel. Top. Quantum Electron. **7**, 703-709 (2001).
15. G.-R. Lin, K.-C. Yu, and Y.-C. Chang, "10 Gbit/s all-optical non-return-to-zero to return-to-zero data format conversion based on a backward dark-optical-comb injected semiconductor optical amplifier," Opt. Lett. **31**, 1376-1378 (2006).
16. G. P. Agrawal and N. A. Olsson, "Amplification and compression of weak picosecond optical pulses bu using semiconductor laser amplifiers," Opt. Lett. **14**, 500-502 (1989).
17. N. Storkfelt, B. Mikkelsen, D. S. Olesen, M. Yamaguchi, and K. E. Stubkjaer, "Measurements of carrier lifetime and linewidth enhancement factor for 1.5-mm ridge-waveguide laser amplifier," IEEE Photon. Technol. Lett. **5**, 657-660 (1993).
18. G.-R. Lin, C.-L. Pan, and K.-C. Yu, "Dynamic chirp control of all-optical format-converted pulsed data from a multi-wavelength inverse-optical-comb injected semiconductor optical amplifier," Opt. Express **15**, 13330-13339 (2007)
19. R. Lang, "Injection locking properties of a semiconductor laser," IEEE J. Quantum Electron. **18**, 976-983 (1982).
20. L. Li, "Static and dynamic properties of injection-locked semiconductor lasers," IEEE J. Quantum Electron. **30**, 1701-1708 (1994).
21. R. Hui, S. Benedetto, I. Monitrosset, "Optical bistability in diode-laser amplifiers and injection-locked laser diodes," Opt. Lett. **18**, 287-289 (1993).
22. K. Petermann, *Laser Diode Modulation and Noise* (Kluwer Academic, Dordrecht, The Netherlands, 1988, (corrected 1991).
23. F. Mogensen, H. Olesen, and G. Jacobsen, "Locking conditions and stability properties for a semiconductor laser with external light injection," IEEE J. Quantum Electron. QE-**21**, pp. 784-793, 1985.
24. R. Hui, A. D'Ottavi, A. Mecozzi, and P. Spano, "Injection locking in distributed feedback semiconductor lasers," IEEE J. Quantum Electron. **27**, 1688-1695 (1991).
25. W. Sharfin, M. Dagenais, "Dynamics of optically switched bistable diode laser amplifiers," IEEE J. Quantum Electron. **23**, 303-308 (1987).

1. Introduction

Injection locking of semiconductor lasers has attracted as an intriguing topic since the early 1980s. Versatile featured investigations were explored on their specific characteristics for applications in optical coherent communication networks [1], such as spectral narrowing [2], noise suppression [3], the chirp reduction under modulation [4], and intrinsic frequency response improvement [5] etc. Similar researches have subsequently been employed to study the optical pulse evolution of vertical-cavity surface-emitting lasers (VCSELs) in a slowly varying envelope approximation.[6] VCSELs offer their low manufacturing cost, partly due to the capability for efficient testing at the wafer level, easily and inexpensively providing wavelength tuning over a relatively large range, emitting a highly circular beam that can be coupled into the optical fiber with very high efficiency. They also offer compact size, high speed, low threshold, and low drive current. Injection locking of vertical-cavity surface-emitting lasers (VCSELs) has been attracted as an intriguing topic since early 1990s for use in a variety of optoelectronic applications, such as Injection-locking of VCSEL arrays [1,5], Polarization switching of VCSELs using injection-locking has been shown [6], and recently the effect has been used for an optical inverter [7]. Since 1994, the effect of spontaneous emission on gain enhancement and threshold reduction of VCSELs has been simulated by Li [3], which has subsequently been demonstrated by Sivaprakasam in 1998. Recently, an all-optical NRZ-to-PRZ data format conversion using the switching between dual transverse modes in the VCSEL was preliminarily proposed [8]. Nonetheless, such a dual-mode switching based data format conversion becomes somewhat impractical to achieve without two DFBLDs with precise wavelengths. In this work, we demonstrate an optically injection induced gain-switching VCSEL based NRZ-to-RZ data format converter with the VCSEL RF-biased at un-lasing condition. The eye histogram, on/off extinction ratio, bit-error-rate (BER) and chirp characteristics of the format converted PRZ data stream are analyzed. The data format conversion results such as transformed PRZ date stream, eye

#89943 - $15.00 USD Received 20 Nov 2007; revised 24 Jan 2008; accepted 2 Feb 2008; published 25 Mar 2008

histogram, on/off extinction ratio, and chirp characteristics are analyzed.

2. Experimental Setup

The injection-locked and gain-switched VCSEL NRZ-to-PRZ converter is illustrated in Fig. 1. The VCSEL is biased with a DC current at 1.3 mA and is synchronously modulated by an RF clock with power of 0 dBm, which is operated at just below threshold condition with externally optical injection. [10] For higher bit-rate transmission, the RF clock driven power and the DC biased level are detuned accordingly to match with the increasing threshold condition of VCSEL. The temperature of the VCSEL is controlled at 25^{o}C with fluctuation of <0.1^{o}C to prevent wavelength drift. Subsequently, the VCSEL is externally injected by optical NRZ data-stream, the threshold current of the VCSEL is simultaneously reduced with the incoming high-level data and the gain-switching of VCSEL is initiated to implement NRZ-to-PRZ data format conversion in VCSEL. The optimized condition for external-injection-induced gain-switching of the VCSEL is investigated (see path (A) in Fig. 1) using a tunable laser (ANDO, AQ4321D). For data conversion analysis, the optical NRZ data-stream is simulated by encoding the TL with an amplified 2^{23}-1 PRBS pattern (with Vamp = 1 V) biased Mach-Zehnder intensity modulator (MZM, JDS Uniphase) at linear region of $V_{drive}=V_{3/2\pi}$ ~ 4.1 V), as shown in the path (B) of Fig. 1. Without external injection, the unlasing VCSEL is appropriately DC biased and synchronously modulated with microwave clock signal at just below threshold condition. In contrast to the previous approach, the VCSEL becomes gain-switching as its threshold current is reduced by an external injection. Under such operation, the VCSEL receives the incoming optical NRZ data with high level and is gain-switched to generate a PRZ "1" bit, whereas the low-level ("0" bit) NRZ data ceases the gain-switching of the VCSEL.The traveling-wave typed SOA based all-optical pulsed RZ converter is shown in Fig. 1.

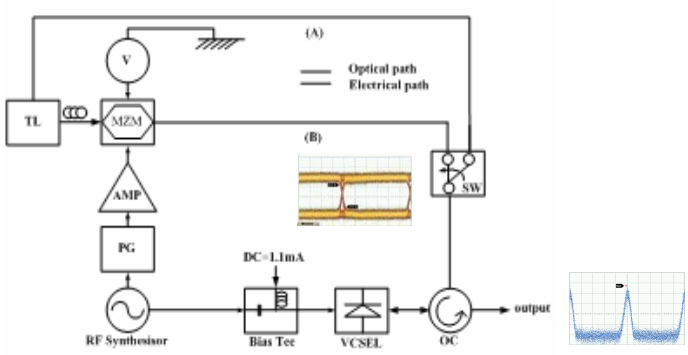

Fig. 1. Setup for the NRZ-to-PRZ format transformer. AMP: power amplifier; VCSEL: Vertical cavity surface emitting laser; MZM: Mach-Zehnder modulator; OC: optical circulator; PC: polarization controller; PG: pattern generator; SW: optical switch; TL: tunable laser.

3. Operation Principle

3.1. Theoretical model

In principle, the threshold current reduction under injection locking condition can be derived by modifying the rate equation of VCSEL gain under external optical injection. In general case, the threshold current of a free-running VCSEL can be written as

$$I_{th}=\frac{qVn_{th}}{\eta_i\tau}, \tag{1}$$

#89943 - $15.00 USD Received 20 Nov 2007; revised 24 Jan 2008; accepted 2 Feb 2008; published 25 Mar 2008

while the relationship between normalized gain and carrier density of VCSEL is described as

$$G(n,S)=\frac{\partial g}{\partial n}v_g\tau_p(n-n_{tr})(1-k_sS)=G_n(n-n_{tr})(1-k_sS), \tag{2}$$

where n is the carrier density in the active region, $\delta g/\delta n$ is the gain coefficient, ν_g is the group velocity of light, τ_p is the photon lifetime, and n_{tr} is the transparent carrier density. The gain is also related to the photon number S in the VCSEL cavity and k_s is the nonlinear gain coefficient. Due to the influence of spontaneous emission, the VCSEL gain is always less than unity, regardless of whether the VCSEL is biased below or above threshold. This gain difference can be then expressed as

$$D_g=G(n,S)-1. \tag{3}$$

Herein, we introduce the concept of the gain compression effect to describe when external light is injecting into the VCSEL. Assuming that the carrier density under external injection is n_{ui} and that the photon number is S_{ui}, the normalized gain is then re-written as

$$G(n_{ui},S_{ui})=G_n(n_{ui}-n_{tr})(1-k_sS_{ui}). \tag{4}$$

Under an externally injection-locking condition, the VCSEL is biased at just below threshold while the gain of VCSEL can be approximately modifies as

$$G(n_{ui},S_{ui})\approx 1+D_g+\delta G=1+D_g+G_n\Delta n-G(n,S)k_s\Delta S, \tag{5}$$

where n_{th} is the threshold carrier density of the free-running laser, $\Delta n = n_{ui} - n \cong n_{ui} - n_{th}$ is the carrier density change due to external light injection, and $\Delta S = S_{ui} - S$. Normally, Eq. (5) can be applied to actual systems which are not biased far below threshold (for example, higher than 95% of their threshold). To include the deviation from threshold, we assume the incremental gain of VCSEL satisfies $|\delta G|<1+D_g$ if the externally injected power is not large. When Eq. (5) is satisfied, the cavity relaxation oscillation frequency $\omega(n_{ui})$ of VCSEL under external injection-locking is given by

$$\omega(n_{ui})=\omega_{th}+\alpha(D_g+G_n\Delta n)/2\tau_p, \tag{6}$$

where α is the linewidth enhancement factor and ω_{th} is the cavity resonance frequency of a free-running laser corresponding to the threshold carrier density n_{th}.[19, 20, 22, 23] By denoting E_{ui} as the internal optical field of the VCSEL, E_i as the optical field of the externally injecting signal, and E_{sp} as the spontaneous emission of the VCSEL, the slowly varying amplitude of the complex electric field E_{ui} in a VCSEL must obey the following rate equation [19 ,20 ,22]

$$\begin{aligned}\frac{dE_{ui}}{dt}&=\left\{j\left[\omega(n_{ui})-\omega_{th}-\Delta\omega_o\right]+\frac{G(n_{ui},S_{ui})-1}{2\tau_p}\right\}E_{ui}+k_cE_i+E_{sp}\\&=\left\{j\left[\frac{\alpha(D_G+G_N\Delta N)}{2}-\Delta\omega_0\right]+\frac{T_G}{2}\right\}E_{ui}+k_cE_i+E_{sp},\end{aligned} \tag{7}$$

with

#89943 - $15.00 USD Received 20 Nov 2007; revised 24 Jan 2008; accepted 2 Feb 2008; published 25 Mar 2008

$$\Delta G = \frac{\delta G}{\tau_p} = \frac{G_n \Delta n - G(n,S)k_s \Delta S}{\tau_p} = \frac{G_n}{\tau_p V}(\Delta n V) - \frac{G(n,S)k_s}{\tau_p}\Delta S = G_N \Delta N - G_S \Delta S, \quad (8)$$

where ΔG denotes the gain change due to external injection, and

$$T_G = D_G + \Delta G, \quad (9)$$

where T_G is the total gain difference of the VCSEL from its threshold value divided by photon lifetime, $G_N=G_n/\tau_p V$, $G_S=G(n,S)k_s/\tau_p$, $\Delta N=\Delta n V$ is the change of carrier number due to optical injection, V is the volume of the active region, $\Delta\omega_0$ is the angular frequency detuning between the free-running and the external injection cases, $D_G=D_g/\tau_p$ and k_c is the coupling coefficient. The steady state condition of the VCSEL can be obtained by assuming $d(\Delta N)/dt=dE_{ui}/dt=0$ [19, 20, 23, 24]. The real and imaginary parts of Eq. (7) can be written together as

$$\frac{(T_G + R_{sp}/S_L)^2}{4} + \left[\frac{\alpha(D_G + G_N \Delta N)}{2} - \Delta\omega_0\right]^2 = \frac{k_c^{\,2}|E_i|^2}{|E_{ui}|^2} = k_c^{\,2}\frac{S_i}{S_L} = S_{iL}, \quad (10)$$

where S_{iL} determines the relative strength of the injection. Therefore, ΔN can be expressed by solving Eq. (10). Obviously, the change of gain, ΔG, reaches its maximum when the frequency detuning $\Delta f_0=\Delta\omega_0/2\pi$ is detuned by Δf_l, [20]

$$\Delta f_l = \left[\frac{\alpha(G_S \Delta S - R_{sp}/S_L)}{2} - k_c\sqrt{(1+\alpha^2)\frac{S_i}{S_L}}\right] \Big/ 2\pi, \quad (11)$$

The frequency Δf_l defines the lower limit of the frequency detuning [20]. Also, the maximum gain variation of VCSEL due to external injection is obtained by substituting Eq. (11) into Eq. (10), as given by

$$\Delta G_m = G_N \Delta N_m - G_S \Delta S_m = -D_G - \frac{R_{sp}}{S_{Lm}} - \sqrt{\frac{4\alpha^2 k_c^{\,2} S_i}{(1+\alpha^2)S_{Lm}}}, \quad (12)$$

where the subscript m means the values corresponding to the maximum gain change. When taking the gain difference D_g (induced by operating the VCSEL at slightly below threshold condition) into consideration by moving the term $-D_g$ to the left-hand side of Eq. (12), we again obtain that the total gain difference $T_g=D_g+\Delta G$ deviated from the threshold value can be increased by the external injection-locking. Note that the gain difference D_g is important only for the free-running VCSEL biased below threshold. The T_g is modified as

$$T_G = D_G + \Delta G_m = D_G + G_N \Delta N_m - G_S \Delta S_m = -\frac{R_{sp}}{S_{Lm}} - \sqrt{\frac{4\alpha^2 k_c^{\,2} S_i}{(1+\alpha^2)S_{Lm}}}, \quad (13)$$

Furthermore, we rewrite Eq. (13) by adding the loss rate $1/\tau_p$ to both sides of it:

$$g = 1/\tau_p + T_G = 1/\tau_p + D_G + \Delta G_m = 1/\tau_p + D_G + G_N \Delta N_m - G_S \Delta S_m$$
$$= \frac{1}{\tau_p} - \frac{R_{sp}}{S_{Lm}} - \sqrt{\frac{4\alpha^2 k_c^{\,2} S_i}{(1+\alpha^2)S_{Lm}}}, \quad (14)$$

The first term on right-hand side of Eq. (14) is the cavity-loss rate for the free-running VCSEL, the second term represents the influence of spontaneous emission, and the last term

#89943 - $15.00 USD Received 20 Nov 2007; revised 24 Jan 2008; accepted 2 Feb 2008; published 25 Mar 2008

represents the effect of external injection on the threshold. It is clear that the external injection effectively reduce the threshold. By including the spontaneous emission part into the rate equation, we can find from Eq. (14) that the threshold gain is significantly reduced from $1/\tau_p$ (free-running) to $[1/\tau_p-R_{sp}/S_{Lm}-(4\alpha^2k_c^2S_i/(1+\alpha^2)S_{Lm})^{1/2}]$ (external injecting). Such a result is opposite to the unchanged threshold condition under external injection ever predicted previously [25], as the threshold gain required to overcome the VCSEL cavity loss is indeed reduced under external light injection. Such an operation of external-injection induced threshold reduction phenomenon is also illustrated in Fig. 2. Finally, the normalized gain at threshold current can also be obtained according to Eq. (2), as expressed by

$$\begin{aligned} G(n_{th},S_{th}) &= \frac{\partial g}{\partial n} v_g \tau_p (n_{th}-n_{tr})(1-k_s S) \approx \frac{\partial g}{\partial n} v_g \tau_p (n_{th}-n_{tr}) \\ &= G_n (n_{th}-n_{tr}) \Rightarrow n_{th} = \frac{G(n_{th},S_{th})}{G_n} + n_{tr} \end{aligned} , \tag{15}$$

By combing Eqs. (14), (15) and (1), we can obtain the reduced threshold current, $I_{th,ui}$, under external injection. In particular, the threshold current is a nonlinear function of the external injection power or photon density, as described by

$$I_{th}' = I_{th} - \frac{eV\tau_{ph}}{G_N\tau_s}\left[\frac{R_{sp}}{S_{Lm}} + \sqrt{4\alpha^2 k_c^2 S_i/(1+\alpha^2)S_{Lm}}\right], \tag{16}$$

where R_{sp} is spontaneous emission rate, S_{Lm} is maximum photon number in the locked mode, α is linewidth broadening factor, k_c is coupling coefficient, and S_i is photon number injected into the laser cavity. This result can be satisfied for versatile laser diode systems.

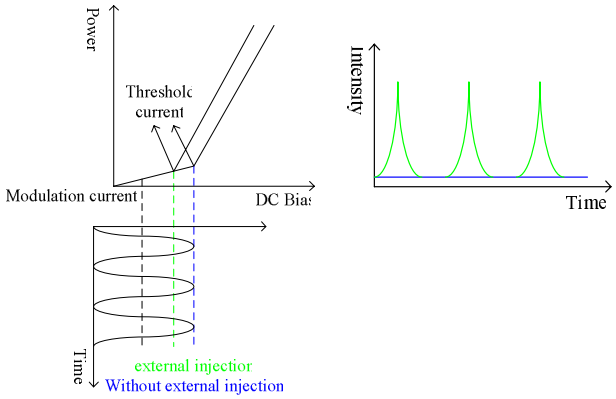

Fig. 2. Left: the operating principle of the gain-switching VCSEL-based NRZ-to-PRZ converter. Right: the output traces of the sinusoidally modulated VCSEL without external injection (Blue) and under an optical injection-locking (Green).

3.2.1 CW external injection

Figure 2 illustrates how the gain switching of is achieved in a bellow-threshold biased and sinusoidally modulated VCSEL under external injection case. (see in Fig. 2). The left figure illustrates the operating principle for the VCSEL-based NRZ-to-PRZ format converter. The right figure illustrates the sinusoidally modulated VCSEL output without external injection and under an optical injection-locking which reduces the threshold to induce gain-switching condition. A higher injection power essentially results in a larger locking range. To investigate the gain-switching of the VCSEL via external optical injection, the VCSEL is bias

#89943 - $15.00 USD Received 20 Nov 2007; revised 24 Jan 2008; accepted 2 Feb 2008; published 25 Mar 2008

at 1.3 mA and modulated by an amplified RF signal of 0 dBm just below the lasing threshold. With an injection power of -21 dBm and a wavelength coincident with that of the VCSEL's fundamental mode, the effective threshold current of the VCSEL will be reduced by the external TL injection. The injection of TL (through optical path (A) in Fig. 1) thus results in the gain-switching of the VCSEL. The pulse-width and peak power of the VCSEL's output are 100 ps and up to 0.3 mW (corresponding to average power of 0.2121 mW).

3.2.2 NRZ-format data external injection

To simulate an incoming data stream with NRZ modulation format, the PG is used to drive a MZM to encode the external injection light, as depicted by optical path (B) in Fig. 1. The MZM (JDS Uniphase; OC-192 Modulator with V_{π}= 4.5 V) is biased at linear operating region. The external-injection-induced gain-switching is initiated when the VCSEL receives the incoming NRZ data stream, providing a transformed PRZ data stream output from the VCSEL. Note that a polarization controller (PC) after the external injection light is used to adjust the polarization of the injection light to match that of the MZM.

4. Results and Discussions

The on/off extinction ratio of the converted PRZ data bit generated from the VCSEL gain-switched by external optical injection is defined as the ratio of the peak power to the noise floor after gain-switching, which is plotted as a function of the external injection power and shown in Fig. 3. The right part in Fig. 3 plots the results obtained for the VCSEL operated under impedance mismatch situation as compared to the impedance matched response. The extinction ratio is greatly degraded with the increasing injection power since the residual optical NRZ data stream partially reflected from the VCSEL end-face is inevitably added into the converted PRZ data stream during the external optical injection case. Our experimental results indicate an optimized extinction ratio of up to 14.7 dB can be obtained at an injection level of -5 dBm. With increasing RF power, the extinction ratio also indicate an increasing trend because the modulated amplitude and slope is concurrently enlarged, however, extremely high RF power could induce a degradation on extinction ratio by linewidth broadening of VCSEL. In contrast, the extinction ratio is of the converted PRZ data from the VCSEL operated at impedance mismatched condition is insufficient to meet the demand of data communication. High injection level although is possible to improve the extinction ratio apparently, which could suffer a risk on optically damaging the VCSEL itself.

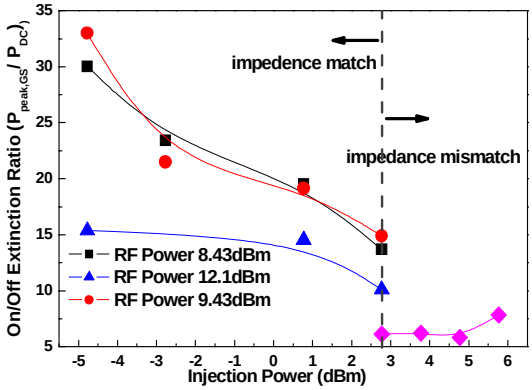

Fig. 3. The extinction ratio ($P_{peak,GS}/P_{DC}$) as a function of injected optical power.

In addition, the degradation on the eye-diagram could be observed since the overlapping of multi-path reflected injection in the VCSEL cavity is concurrently occurred. Adding the RF and optical powers at 0 dBm and -21 dBm, respectively, under impedance matched condition is the best solution to transfer the incoming optical NRZ data stream substantially. Eye

#89943 - $15.00 USD Received 20 Nov 2007; revised 24 Jan 2008; accepted 2 Feb 2008; published 25 Mar 2008

histograms of the input NRZ and converted PRZ data are comparing. The NRZ eye-pattern exhibits rise/fall time, timing jitter, and SNR of 66 ps, 3.4 ps, and 12.5 dB, respectively. After NRZ-to-PRZ conversion, a PRZ data bit with shortened rise time of 53 ps is obtained, however, the enlarged fall-time and timing jitter, and the degraded SNR of 100 ps and 5.1 ps, and 9.2 dB, respectively, are concurrently observed from 3 GHz receiver. Such a degradation inevitably occurs under the initial condition of the VCSEL at below threshold. Note that the dc level of NRZ is smaller than that of the RZ as the VCSEL induces additional spontaneous emission noise into converted signal, while the reflection of NRZ at the surface of the cavity may also be a contributed factor to the bad SNR (see in Fig. 2). In addition, the pattern effect increases as a result of the temporally varied carrier concentration in the VCSEL. Figure 4 illustrates two specific RZ data streams output from the VCSEL based NRZ-to-PRZ converter after fine tuning PC and external injection wavelength respectively. A slightly unequalized pattern amplitude occurs due to the insufficient recovering time for the gain of VCSEL operated at beyond 1.25 Gbit/s. Without a strong injection or feedback, such a pattern effect under continuous gain-switching operation is unable to be removed due to the intrinsic limitation on gain and bandwidth characteristic of the VCSEL with quantum dot based active layer structure. Nonetheless, the injection level is another important issue during operation as which could seriously damage the VCSEL prior to improve its frequency response.

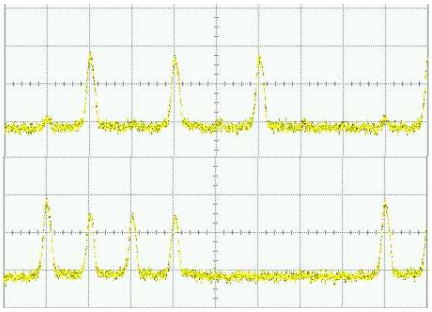

Fig. 4. The "01010100" and "11110000" RZ data streams converted by the gain-switched VCSEL.

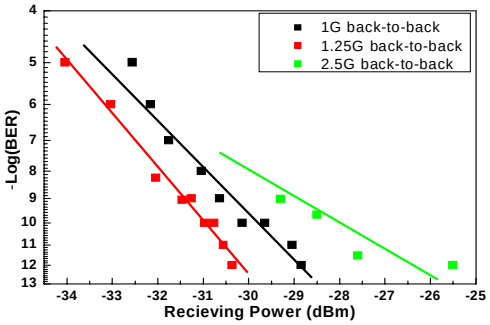

Fig. 5. The back-to-back transmission BER of the converted RZ PRBS data stream at 1 and 1.25 Gbit/s.

On the other hand, the BER analyses of the converted RZ PRBS data stream are shown in Fig. 5. The least optical receiving power for a BER of 10^{-9} is -29 dBm at 2.5 Gbit/s, A positive power penalty of up to 2 dB is observed when increasing the data bit-rate from 1 to 2.5 Gbit/s. Such a gain-switching operation further helps to improve on/off extinction ratio and bit error rate (BER) of the incoming NRZ PRBS signal under detuning of the DC biased level of the VCSEL at different optically injection levels. The source of power penalties that can lead to sensitivity degradation can be separated by three categories. The degraded extinction ratio due to the residual signal occurred at 0 bit inevitably gives rise to an enlarged increasing BER. Which can also be contributed by the intensity noise of the VCSEL with instability. In comparison with the eye-pattern of RZ data streams shown in Figs. 5, 6, and 7 (which has been converted with a specially RZ-to-NRZ receiver), it is obtained that the timing jitter designed is enlarged from 16ps to 21ps as the transmission data rate increases from 1 to 2.5 Gbit/s. In addition, the frequency chirp induced by fiber dispersion and spectral broadening will also affected the eye-pattern and result in additional noises.

#89943 - $15.00 USD Received 20 Nov 2007; revised 24 Jan 2008; accepted 2 Feb 2008; published 25 Mar 2008

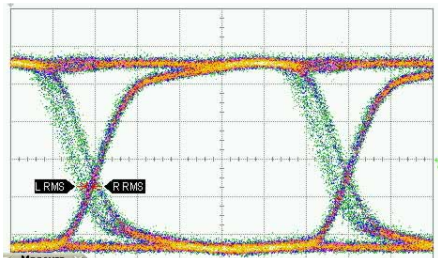

Fig. 6. The eye diagram of 1 G.bit/s at BER 10^{-8}.

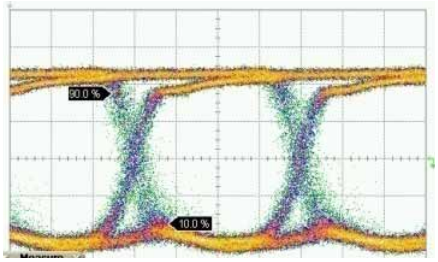

Fig. 7. The eye diagram of 2.5 G.bit/s at BER 10^{-7}

The frequency chirp of the VCSEL converted RZ data derived from the phase modulation is positive at the rising edge ($\delta\varphi/\delta t < 0$) and negative at the falling edge ($\delta\varphi/\delta t > 0$), thus leading to a negative peak-to-peak chirp parameter C. Without appropriate compensation, such a chirp variation inevitably broadens the pulsed RZ data after propagating in a medium with a positive dispersion parameter D. The traces and corresponding frequency chirps of the converted pulsed RZ data stream at continuous "on" and discrete "on" conditions are compared and shown in Fig. 8. The peak-to-peak chirp of the gain-switched VCSEL based NRZ-to-RZ data converter is 4.47 GHz and 6.5 GHz at bit rates of 1 Gbit/s and 2.5 Gbit/s, respectively. Under the injection of continuous "on" data with average power of 0 dBm and duty-cycle of 25%, the peak-to-peak chirp of the converted pulsed RZ signal is 241 MHz/ps. The chirp of RZ data significantly increases to 178 MHz/ps as the data bit-rate decreases, which is directly correlated with the transient gain property of the VCSEL during NRZ-to-RZ conversion.

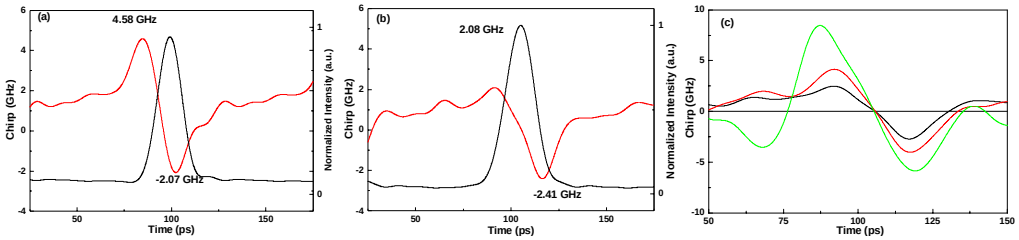

Fig. 8. Traces and Chirp of converted pulsed RZ signal of single-wavelength injection with continuous (a) and data (b), (c) are corresponding chirps at receiving powers of 0 dBm (black-line), -1dBm (red-line) and -2 dBm (green line).

Previously, our group has also demonstrated an all-optical NRZ-to-RZ data format converter using a backward dark-optical-comb injected SOA [18], its degraded power penalty performance is subject to the net effect of addition chirp and dispersion. Under the injection of multi- and single-wavelength inverse-optical-combs, the peak-to-peak chirp of the converted pulsed RZ signal from the SOA are up to 11.9 GHz and 13.2 GHz, respectively. Furthermore, the FWHM of the multi- and single-wavelength injection converted pulsed RZ data from SOA are about 31 ps. In comparison with the previous work on the SOA based NRZ-to-RZ converter, our VCSEL based NRZ-to-RZ converter has already indicating a better performance on the reduction of the peak-to-peak chirp by a factor of 3.

5. Conclusion

In conclusion, all-optical NRZ-to-RZ data transform conversion by optical injection VCSEL are demonstrated. The extinction ration of the VCSEL based NRZ-to-RZ transformer is found to strongly correlated with the external injection power and RF power. The optimized RF power of 0 dBm and the external injection power of -21 dBm and DC current of 1.3 mA is determined. The maximum on/off extinction ratio is 9 dBm and the pulsewidth is 100 ps. In addition, with decreasing the external injection power, the pattern effect will be improved.

#89943 - $15.00 USD Received 20 Nov 2007; revised 24 Jan 2008; accepted 2 Feb 2008; published 25 Mar 2008

In comparison with single-wavelength injection with continuous and data, single-wavelength with data injection exhibits better frequency-chirp reduction performance.

Acknowledgment

This work is partially supported by the National Science Council of Republic of China under grants NSC96-2221-E-002-099 and NSC96-2752-E-009-008-PAE.

#89943 - $15.00 USD Received 20 Nov 2007; revised 24 Jan 2008; accepted 2 Feb 2008; published 25 Mar 2008